RAPID COMMUNICATIONS

PHYSICAL REVIEW D VOLUME 36, NUMBER 10 15 NOVEMBER 1987

Space structure of confining strings

J. Wosiek* and Richard W. Haymaker
Department of Physics and Astronomy, Louisiana State University, Baton Rouge, Louisiana 70803
(Received 24 June 1987)

The energy density of the chromoelectric field generated by the static $q\bar{q}$ pair is computed in the SU(2) lattice gauge theory. The energy density in the central region of the Wilson loop shows significant deviations from the Coulomb behavior and approaches a constant value at $R_{q\bar{q}}=0.8-1.1$ fm.

Monte Carlo studies of the space structure of the non-Abelian strings are customarily done by measuring the energy density in the presence of a static $q\bar{q}$ pair. On the lattice it is approximated by the correlation function[1-3]

$$\rho_W(x)=\frac{\langle WP_x\rangle-\langle W\rangle\langle P\rangle}{\langle W\rangle}\ . \tag{1}$$

This technique, however, is limited by the rapid falloff of the expectation value of the Wilson loop W as we move toward larger separations of the static $q\bar{q}$ pair. The source of this difficulty is well understood, and, unfortunately, no satisfactory solution of this problem has been proposed yet. The ultimate algorithm should generate field configurations corresponding to a source and sink at the $q\bar{q}$ locations. This is not available in non-Abelian lattice gauge theories. Hence we must use the Wilson loop in Eq. (1) to project the required field configurations out of all possible ones generated by the standard lattice Monte Carlo.

We have pushed up the attainable $q\bar{q}$ separations by modifying the brute-force method in the direction required by the ideal algorithm. To this end we propose to measure, instead of the numerator in Eq. (1), the difference

$$\delta_W(x)=\langle WP_x-WP_\infty\rangle\ , \tag{2}$$

where the position of the reference plaquette P_∞ is chosen such that the correlation function already factorizes $\langle WP_\infty\rangle\cong\langle W\rangle\langle P\rangle$. In practice this happens well within the volume available with present lattices. The reason this gives an improvement is simple: while giving the same average, the difference in Eq. (2) fluctuates less, since the main fluctuations of the product WP come from the W itself. This extremely simple modification reduces fluctuations due to the projector, and hence more closely approximates the ideal algorithm.

The above trick reduced statistical errors by a factor of 10. Together with the multihit measurements, we diminished fluctuations by a factor of 15, which allowed us to measure δ_W for W's up to 6×6 at $\beta=2.5$. For the first time one can study the energy distribution in the "central region" of the Wilson loop, where confining strings should be directly seen.

We have simulated pure SU(2) Yang-Mills theory on a 14×15^3 lattice, in the $\beta(=4/g^2)$ range $2.3\le\beta\le2.5$. Correlations of the $M\times M$ Wilson loop and elementary plaquettes were measured for $3\le M\le6$. Some data on the 7×7 loop were also taken; however, they serve only as an illustration of the string instabilities caused by the finite size of the lattice (see below).

Field configurations were generated using the SU(N) program of Creutz which was kindly made available to us by the author. Creutz's recent modification of the Metropolis algorithm was implemented. It reduces significantly sweep-to-sweep correlations by exploiting the freedom in the choice of the Metropolis proposition U' (Ref. 4).

To decrease statistical errors further, we have used the analytic version of the multihit measurement technique proposed by Parisi *et al.*[5] In the case of the measurement of the Wilson loop one replaces

$$W=\prod_{l\in\Gamma}U_l\rightarrow\overline{W}=\prod_{l\in\Gamma}{}'\,\overline{U}_l \tag{3}$$

in the measured quantity, where

$$\overline{U}_l=\frac{\int U_l\exp\left[\frac{1}{g^2}\mathrm{Tr}(U_lX_l^\dagger+\mathrm{H.c.})\right]dU_l}{\int\exp\left[\frac{1}{g^2}\mathrm{Tr}(U_lX_l^\dagger+\mathrm{H.c.})\right]dU_l}$$
$$=X_l\frac{I_2(\beta\lambda)}{\lambda I_1(\beta\lambda)}\ , \tag{4}$$

where $\lambda=\sqrt{\det(X)}$ and where $X_l^\dagger$ is the neighborhood of U_l, i.e., $U_lX_l^\dagger=\sum_{P\ni l}U_P$, and the summation extends over all plaquettes containing the link l. It is well known that this prescription gives the same $\langle W\rangle$ if the one link adjacent to each corner of W is left unmodified.[5,6] In the case of the correlation $\langle WP\rangle$, the same idea applies: $\langle\overline{W}P\rangle=\langle WP\rangle$ provided P does not have links common with W. One could modify the replacement, Eq. (3) such that it applies also when W and P overlap. However since the continuum energy density is not well defined along the $q\bar{q}$ world line anyway, we have measured $\langle\overline{W}P\rangle$ and used only nonoverlapping configurations for further analysis.

Depending on β and the size of W, the multihit technique reduces errors by a factor 2–5. Together with our choice, Eq. (2) for the measured object, we reduced fluctuations by a factor of 15 while increasing the CPU time only by 60%. Overall efficiency of our algorithm is therefore 140. This substantial reduction of the noise al-

lowed us to perform all the computations on the FPS-264 vector computer which is approximately ten times slower than the Cyber 205 in our application.

Figure 1 shows our raw data for the correlations $\delta_W(x)$ as a function of a position of a plaquette P, for various sizes of W. Only $E_\parallel{}^2$ was measured; hence, P was always kept parallel to the W plane. Transverse distances are set to zero and the time slice is taken to lie in the middle of W.

The existence of the non-Abelian flux is well established inside all measured loops. Note however the change of the vertical scale as we move to larger loops. Bearing in mind the bias introduced by the multihit measurement, we will use only the data from the middle bins of Fig. 1 for the subsequent analysis.

It is apparent, from Fig. 1, that the short-distance Coulomb-type contributions dominate.[2] (Unbiased, by the multihit procedure, data show yet larger peaks around the $q\bar{q}$ positions.) Only for larger loops ($M=5,6$) they become separated sufficiently to reveal the central region. To check the scaling we have plotted the energy density in the central region

$$\epsilon(R)=\beta\frac{\delta_W\left[\frac{M}{2},\frac{M}{2},0,0\right]}{a^4\langle W\rangle} \tag{5}$$

as the function of the $q\bar{q}$ separation R. Contributions from other components of the E and B fields were neglected in accordance with the findings of other authors.[1,2] Figure 2 shows our results for ϵ plotted versus R in physical units. We have used $\Lambda_L/\sqrt{\sigma}=0.013$, $\sqrt{\sigma}=0.42$ GeV in order to fix a scale of the lattice constant a (Ref. 1). Not surprisingly, data from the 3×3 loops do not scale, especially for smaller β. On the other hand, 4×4 points, together with the correlations with the bigger loops, seem to cluster around the common line. To achieve this agreement however, we had to include the "geometrical correction factor" for the (even×even) loops which was the same for all three β values, and agrees with the one introduced for 4×4 loop by Fukugita and Nyuia ($\delta=1.44$) in their analysis of the transverse distributions.[1] We have found that the correction needed for the 6×6 loop is smaller ($\delta=1.05$) confirming their finite-size nature. Geometrical interpretation of these factors was discussed in Refs. 1 and 7.

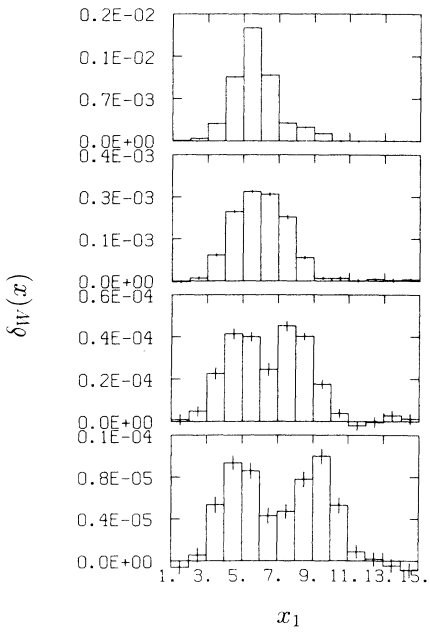

FIG. 1. Correlation function, Eq. (2) as the function of the position of the plaquette x_1 in lattice units, for the $q\bar{q}$ separation varying from 3 (top) to 6 (bottom). One quark is always located at $x_1=4$.

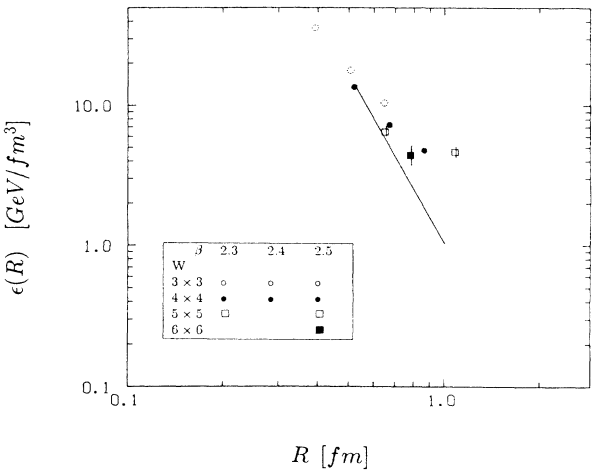

FIG. 2. The energy density Eq. (5) as a function of the $q\bar{q}$ separation R in physical units. Solid line represents arbitrarily normalized Coulomb prediction.

Given the approximate scaling, the universal function $\epsilon(R)$ allows to distinguish between the Coulomb versus linear nature of the energy density in the central region. Even at small $q\bar{q}$ separation it falls slower ($\sim R^{-3}$) than the canonical ($\sim R^{-4}$) Coulomb contribution. Slow ($\sim R^{-2}$) dependence, at these separations, emerges naturally if strings expand linearly in the transverse directions while maintaining constant σ. Such a behavior was indeed found earlier,[1] and is consistent with our analysis of the transverse directions (see below). For larger R, $\epsilon(R)$ seems to flatten at $R_{q\bar{q}}=0.8-1.1$ fm (Ref. 8). Finally, the total energy contained in the one unit of the transverse slice of the string is compatible with the string tension measured independently by other authors.[6,9,10]

The energy density falls rapidly in the directions transverse to the W plane. In our β range, correlations, Eq. (2), practically vanish for transverse separations larger than four lattice units, with large statistical errors at $x_\perp=3$. Consequently, the mean-square thickness of the string[1,7]

$$\alpha^2(x_1,x_2)=\frac{\int x_\perp{}^2\epsilon(x_\mu)d^2x_\perp}{\int\epsilon(x_\mu)d^2x_\perp} \tag{6}$$

is not well determined, since it is sensitive to the poorly

known values of ϵ at larger $x_\perp$. In the limited range of $x_\perp$, where our data are available, the energy distribution is exponential rather than Gaussian. Therefore, instead of Eq. (6), we have measured the discretized version of the logarithmic derivative at the origin

$$b_0^{-1}=\ln\left[\frac{\epsilon\left[\frac{M}{2},\frac{M}{2},0,0\right]}{\epsilon\left[\frac{M}{2},\frac{M}{2},\hat{\mathbf{e}}_\perp\right]}\right] \tag{7}$$

which is more stable and also provides some, though necessarily limited, information about the $x_\perp$ dependence. Figure 3 shows b_0 plotted versus R in physical units. Again data from the small (3×3) loops do not scale, while larger loops seem to follow a common line. Similarly to the previous case, $\epsilon(M/2,M/2,0_\perp)$ for the 4×4 and 6×6 loops required multiplicative correction which turned out to be the same as before.

The precise relation between b_0 and α is unknown and reflects our ignorance of the large-$x_\perp$ region. If the exponential falloff continues, for the intermediate $x_\perp$, our value of b_0 would give $\alpha\sim1$ fm. In this case the direct use of the definition Eq. (6) coupled with the lattice limitations severely underestimates mean thickness. For example, only 10%–50% of the *second moment* is obtained from the typically accessible $x_\perp$ range of $(1-3)b_0$. This explains very small values of α quoted in Ref. 1. Only if we can reach the $x_\perp$ range, where the Gaussian profile shows up,[11,12] one could use definition (6) with more confidence. Exponentially diffused, at intermediate $x_\perp$, flux tubes may offer a simple reconciliation of the two rather different scales appearing in this context. While giving typically hadronic, *mean thickness* (1 fm), they also account for the thin (0.2–0.4 fm), in the sense of the total energy deposition, strings seen in the present lattice calculations. The zeroth and the second moments of the exponential distribution acquire contribution from vari-

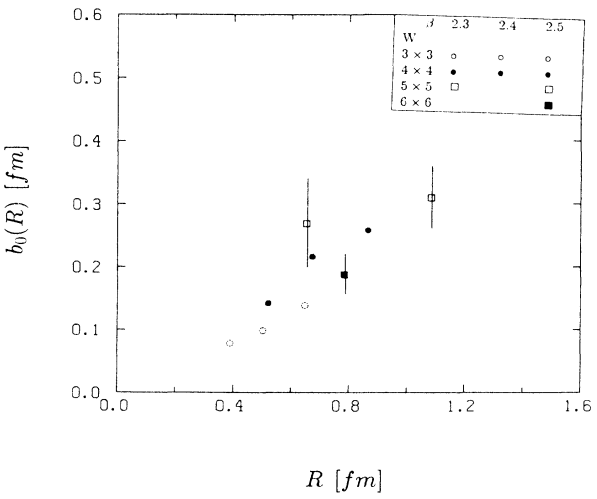

FIG. 3. The inverse slope of the exponential $x_\perp$ distribution plotted versus R in physical units.

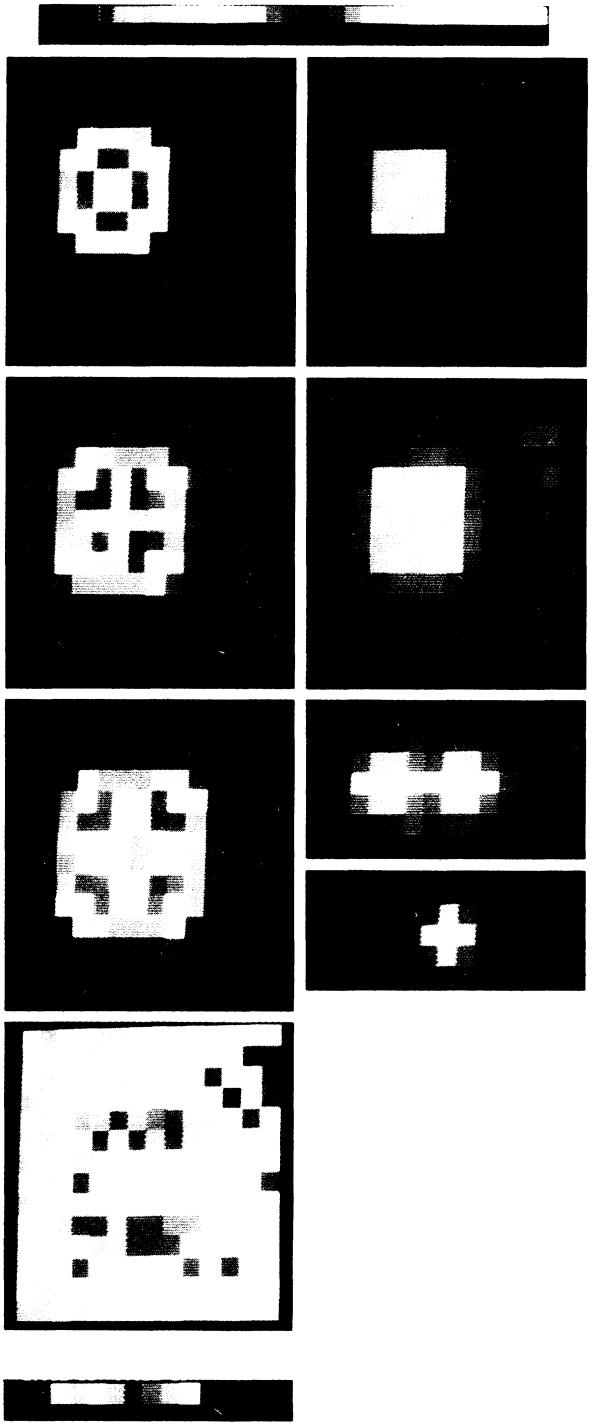

FIG. 4. Color maps of the energy distribution at $\beta=2.5$. Wilson loop size varies from 4×4 [top row (1)] to 7×7 [bottom row (4)]. First column: the Wilson loop is in the displayed plane. Second column: the displayed plane is separated from W (of size 4×4 and 5×5, respectively) by one lattice unit in the transverse direction; "static view," and the "transverse section" of the $q\bar{q}$ string for the $q\bar{q}$ distance equal to 6.

ous $x_\perp$ regions explaining above difference.

Finally we would like to mention the usefulness of the "color maps," when presenting results of the lattice simulations. It is often emphasized that one of the problems of the large-scale simulations is the huge amount of the data which is difficult to present concisely. While nothing can beat the regular statistical analysis of *a particular relation,* clear qualitative representation of the multidimensional function is also important. Figure 4 shows a series of the two-dimensional sections through our hypercubic lattice with the value of the correlation function, Eq. (2) represented by a color chosen accordingly to the enclosed linear scale. The color scale at the top runs from -1.5×10^{-5} to 4.1×10^{-4} for row 1, -5.6×10^{-6} to 1.1×10^{-4} for row 2, and -1.8×10^{-6} to 2.6×10^{-5} for row 3. The color scale at the bottom is for row 4 running from -1.9×10^{-6} to 5.5×10^{-6}. Typical errors for rows 1 through 4 are, respectively, 5×10^{-6}, 3×10^{-6}, 7×10^{-7}, and 7×10^{-7}. We have found such maps very useful in the initial stage of the analysis. For example, the dramatic effect of the finite size of the lattice is immediately seen when comparing energy distributions for 6×6 and 7×7 loops (rows 3 and 4). (The change of colors was chosen to correspond to the variation of δ_W by one standard deviation. This explains fewer colors in row 4.) Emergence of the central region inside the Wilson loop is clear and helps in choosing data for further more precise analysis. Symmetry under rotations in the W plane is also more readily seen from Fig. 4 than from appropriate histograms. Yet another example, is the clear effect of the multihit procedure on the short-distance part of δ_W. Plaquettes attached to the four links unaffected by the substitution (3) are easy to recognize. Study of the more subtle effects such as the string fluctuations might be possible in the not so distant future.

We would like to thank M. Creutz for providing his program generating lattice configurations. We also thank R. Caldi, M. Creutz, and C. Rebbi for discussion. This work was supported in part by the U.S. Department of Energy under Contract No. DE-AS05-77ER05490.

---

*On leave of absence from the Jagellonian University, Kraków, Poland. Present address: Institute of Physics, ul Reymonta 4, Kraków, Poland.

[1]M. Fukugita and I. Niuya, Phys. Lett. **132B**, 374 (1983).

[2]J. Flower and S. Otto, Phys. Lett. **160B**, 128 (1985); see also J. Flower, Caltech Report No. CALT-68-1378-mc, 1986 (unpublished).

[3]D. G. Caldi, in Proceedings of the Lattice Gauge Theory Conference, Upton, New York, 1986, edited by H. Satz (Plenum, New York, to be published).

[4]M. Creutz, Phys. Rev. D **36**, 515 (1987); Report No. BNL-39747, 1987 (unpublished).

[5]G. Parisi, R. Petronzio, and F. Rapuano, Phys. Lett. **128B**, 418 (1983).

[6]C. Lang and F. Karsch, Phys. Lett. **138B**, 176 (1984).

[7]R. Sommer, thesis, Wuppertal Report No. WUB 86-13, 1986 (unpublished).

[8]J. D. Bjorken, Phys. Rev. D **27**, 140 (1983).

[9]A. Billoire and E. Marinari, Phys. Lett. **128B**, 399 (1984).

[10]F. Gutbrod, Z. Phys. C **30**, 585 (1986).

[11]M. Lüscher, G. Münster, and P. Weisz, Nucl. Phys. **B180 [FS2]**, 1 (1981).

[12]C. Peterson and L. Sköld, Nucl. Phys. **B255**, 365 (1985).

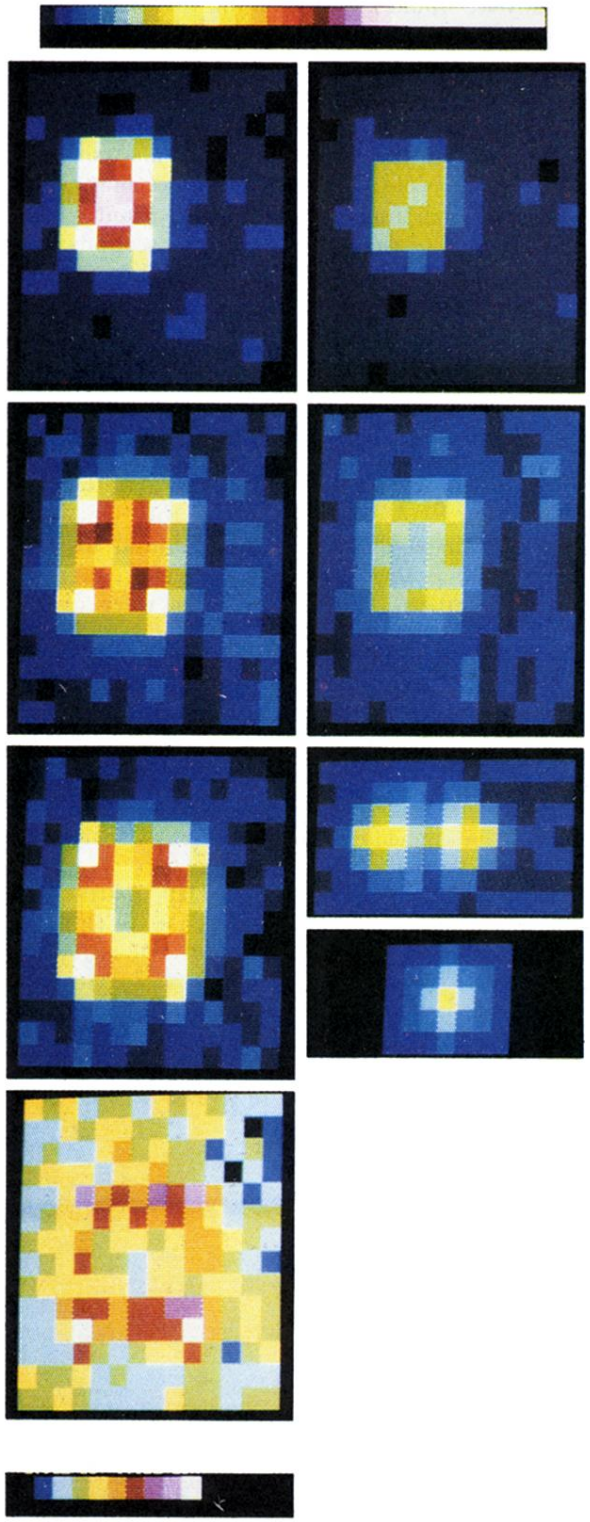

FIG. 4. Color maps of the energy distribution at $\beta=2.5$. Wilson loop size varies from 4×4 [top row (1)] to 7×7 [bottom row (4)]. First column: the Wilson loop is in the displayed plane. Second column: the displayed plane is separated from W (of size 4×4 and 5×5, respectively) by one lattice unit in the transverse direction; "static view," and the "transverse section" of the $q\bar{q}$ string for the $q\bar{q}$ distance equal to 6.